AD-A240 831

1-f BINARY JOINT TRANSFORM CORRELATOR

Kenneth H. Fielding, Capt, USAF and Joseph L. Horner
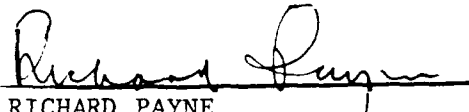
DTIC
ELECTE
SEP 10 1991
S D
D

91-10972

This report has been reviewed by the RADC Public Affairs Division (PA) and is releasable to the National Technical Information Services (NTIS). At NTIS it will be releasable to the general public, including foreign nations.

RADC-TR-90-201 has been reviewed and is approved for publication.

APPROVED:

RICHARD PAYNE
Chief, Electro-Optic Device Technology Division
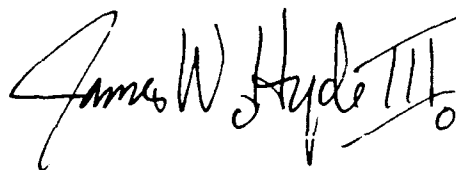Directorate of Solid State Sciences

APPROVED:

HAROLD ROTH
Director of Solid State Sciences

FOR THE COMMANDER:

JAMES W. HYDE III
Directorate of Plans & Programs

If your address has changed or if you wish to be removed from the RADC mailing list, or if the addressee is no longer employed by your organization, please notify RADC (ESOP) Hanscom AFB MA 01731-5000. This will assist us in maintaining a current mailing list.

Do not return copies of this report unless contractual obligations or notices on a specific document require that it be returned.

REPORT DOCUMENTATION PAGE

Public reporting for this collection of information is estimated to average 1 hour per response, including the time for reviewing instructions, searching existing data sources, gathering and maintaining the data needed, and completing and reviewing the collection of information. Send comments regarding this burden estimate or any other aspect of this collection of information, including suggestions for reducing this burden, to Washington Headquarters Services, Directorate for Information Operations and Reports, 1215 Jefferson Davis Highway, Suite 1204, Arlington, VA 22202-4302, and to the Office of Management and Budget, Paperwork Reduction Project (0704-0188), Washington, DC 20503.

1. AGENCY USE ONLY (Leave blank)	2. REPORT DATE	3. REPORT TYPE AND DATES COVERED
	July 1990	In-House 1 Nov 89 to 31 Mar 90

4. TITLE AND SUBTITLE

1-f Binary Joint Transform Correlator

5. FUNDING NUMBERS

PE 61102F
PR 2305
TA J7
WU 11

6. AUTHOR(S)

Kenneth H. Fielding Capt., USAF; Joseph L. Horner

7. PERFORMING ORGANIZATION NAME(S) AND ADDRESS(ES)

Rome Air Development Center
RADC/ESOP
Hanscom AFB
Massachusetts 01731-5000

8. PERFORMING ORGANIZATION REPORT NUMBER

RADC-TR-90-201

9. SPONSORING/MONITORING AGENCY NAME(S) AND ADDRESS(ES)

10. SPONSORING/MONITORING AGENCY REPORT NUMBER

11. SUPPLEMENTARY NOTES

12a. DISTRIBUTION/AVAILABILITY STATEMENT

Approved for public release; distribution unlimited

12b. DISTRIBUTION CODE

13. ABSTRACT (Maximum 200 words)

A 1-f lens focal length binary joint transform correlator is described. This correlator uses a magneto-optic spatial light modulator, lens, and standard 8-bit resolution CCD camera. Computer simulations and experimental results of the effects of changes in scale, in-plane rotation, out-of-plane rotation, target/reference separation, and multiple targets are discussed. The performance using actual sensor imagery containing clutter is presented.

14. SUBJECT TERMS

Joint transform correlator, Binary joint transform correlator, Pattern recognition, Information processing

15. NUMBER OF PAGES

34

16. PRICE CODE

17. SECURITY CLASSIFICATION OF REPORT	18. SECURITY CLASSIFICATION OF THIS PAGE	19. SECURITY CLASSIFICATION OF ABSTRACT	20. LIMITATION OF ABSTRACT
Unclassified	Unclassified	Unclassified	SAR

NSN 7540-01-280-5500

Preface

We would like to thank Lieutenant Charles Makekau for his support with the computer programming. We also thank Major (Dr.) Steve Rogers of the Air Force Institute of Technology and Dr. Bahram Javidi of the University of Connecticut for their enlightening discussions.

Contents

Illustrations

1-f Binary Joint Transform Correlator

1. INTRODUCTION

Since the inception of the joint transform correlator[1] (JTC), many researchers, mostly through computer simulation and some experimentation, have shown this correlator architecture can produce good correlation performance.[2,3,4] Javidi proposed binarizing the joint Fourier transform power spectrum[5] (JPS) and later extended it to a kth law non-linearity[6,7] revealing a family of correlation types ranging from the JTC for $k = 1$, to the

[1] Weaver, C.S., and Goodman, J.W. (1966) A technique for optically convolving two functions, *Appl. Opt.*, **5**:1248.

[2] Florence, J. (1989) Joint-transform correlator systems using deformable-mirror spatial light modulators, *Opt. Lett.*, **14**:341.

[3] Hudson, T. and Gregory, D. (1990) Joint transform correlation using an optically addressed ferro electric liquid crystal spatial light modulator, *Appl. Opt.*, **29**:1064.

[4] Yu, F.T.S., Jutamulia, S., Lin, T.W., and Gregory, D.A. (1984) Adaptive real-time pattern recognition using a liquid crystal TV based joint transform correlator, *Appl. Opt.*, **26**:1370.

[5] Javidi, B., and Kuo, C. (1988) Joint transform image correlation using a binary spatial light modulator at the Fourier plane, *Appl. Opt.*, **27**:663.

[6] Javidi, B. (1989) Nonlinear joint power spectrum based optical correlation, *Appl. Opt.*, **28**:2358.

[7] Javidi, B., and Horner, J.L. (1989) Multifunction nonlinear signal processor: deconvolution and correlation, *Opt. Eng.*, **28**:837.

binary joint transform correlator (BJTC) for k = 0. The correlations of the original JTC (k = 1) correspond to a classical matched filter, k = 1/2 to the phase-only filter, and k = 0 to the inverse filter. A binary spatial light modulator (SLM) is sufficient to implement k = 0 whereas a greyscale SLM is required for higher values of k. Compared to the classical JTC, the BJTC provides significantly higher peak intensity, larger peak-to-secondary ratio, delta-like correlations, and better cross-correlation discrimination.[2,3,4,5,6,7,8,9] The intention of this work is twofold: to show a method that allows a standard 8-bit greyscale detector to accurately capture the JPS, and to experimentally characterize the BJTC performance for the cases of object separation, in-plane rotation, out-of-plane rotation, scale, multiple targets, and clutter.

2. BACKGROUND

The usual method of implementing the JTC uses two identical systems that includes a SLM, Fourier transform (FT) lens, and a CCD camera. The first system generates the JPS which is operated on by some kth law nonlinearity and passed to the second system to generate the correlation. This method requires two of every component and can be quite expensive. Architectures have been proposed that use a single system and time share the JPS generation and correlation steps.[8,9] We propose a system combining the variable scale correlator architecture[10,11,12] with the single SLM architecture[9] and a dc block to arrive at the 1-f joint transform correlator architecture shown in Figure 1.

---

[8] Javidi, B., and Horner, J.L. (1989) Single spatial light modulator joint transform correlator. *Appl. Opt.*, **23**:1027.

[9] Javidi, B., Gregory, D.A., and Horner, J.L. (1989) Single spatial light modulator joint transform correlator architectures. *Appl. Opt.*, **28**:411.

[10] Makekau, C., and Horner, J.L. (1990) 2-f optical correlator. *Appl. Opt.*, **29**.

[11] Goodman, J.W. (1968) *Introduction to Fourier Optics*, McGraw-Hill, San Francisco.

[12] Vander Lugt, A. (1966) Practical considerations for the use of spatial carrier-frequency filter. *Appl. Opt.*, **5**:1760.
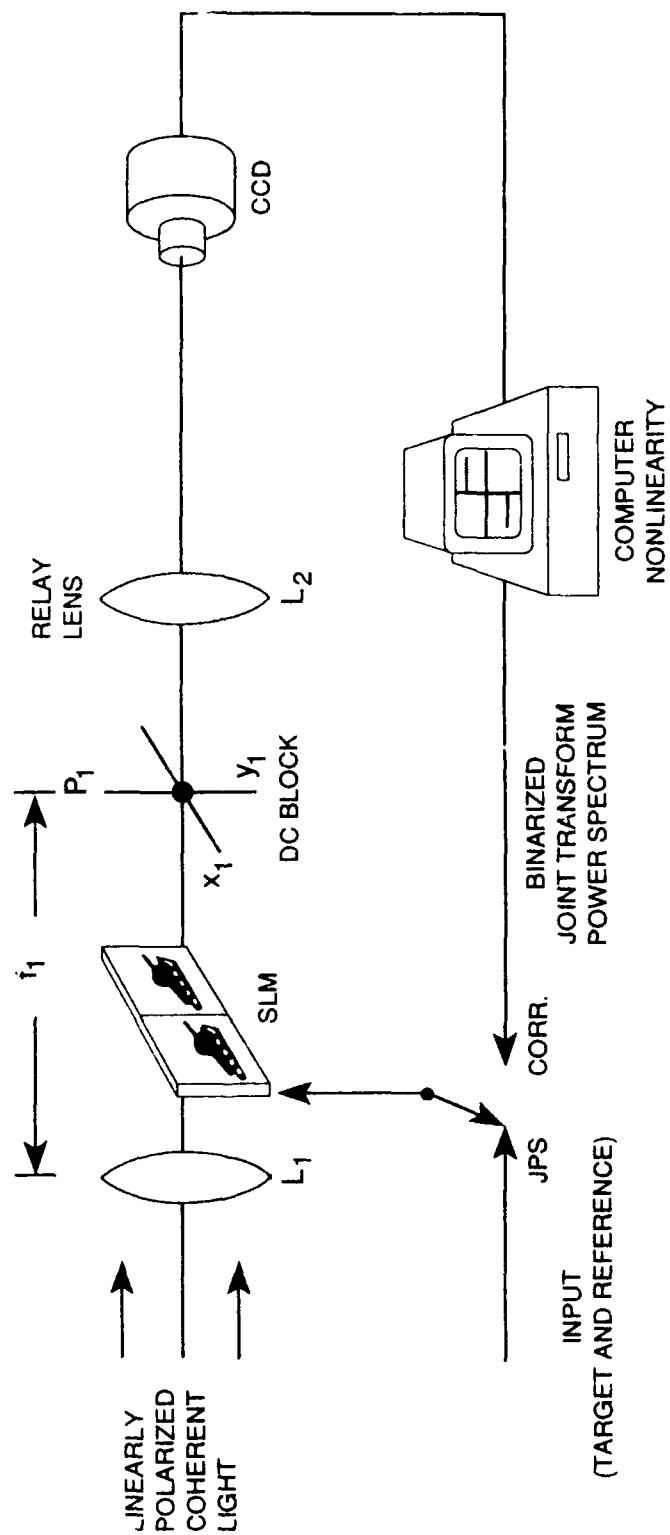
Figure 1. 1-f Binary Joint Transform Correlator.

In either configuration, the reference and target signals are placed on their respective halves of the input SLM and are denoted by $r(x + x_0, y)$ and $s(x - x_0, y)$. The complex field at the Fourier plane, P_1 in Figure 1, is given by

$$U(\alpha,\beta) = \{ \; S(\alpha,\beta) \exp(i\phi_s(\alpha,\beta)) \exp(-ix_0\alpha)$$

$$+ R(\alpha,\beta) \exp(i\phi_R(\alpha,\beta)) \exp(ix_0\alpha) \} \exp\left(\frac{ik}{2d}(\alpha^2 + \beta^2)\right) \tag{1}$$

where (α, β) are the angular spatial frequency coordinates, $R(\alpha,\beta) \exp(i\phi_R(\alpha,\beta))$ and $S(\alpha,\beta) \exp(i\phi_S(\alpha,\beta))$ are Fourier transforms of the reference $r(x, y)$ and target $s(x, y)$, and the last term is a quadratic phase factor.[11] The interference intensity is given by

$$I(\alpha, \beta) = S^2(\alpha, \beta) + R^2(\alpha, \beta)$$

$$+ S(\alpha, \beta) \exp(i\phi_S(\alpha, \beta)) R(\alpha, \beta) \exp(-i\phi_R(\alpha, \beta) \exp(-i2x_0\alpha)$$

$$+ S(\alpha, \beta) \exp(-i\phi_S(\alpha, \beta)) R(\alpha, \beta) \exp(i\phi_R(\alpha, \beta) \exp(i2x_0\alpha). \tag{2}$$

Classically (for $k = 1$), the Fourier transform of the above equation produces the auto and cross-correlation signals given by

$$h(x_1, y_1) = R_{R,R}(x_1, y_1) + R_{S,S}(x_1, y_1) R_{R,S}(x_1 - 2x_0, y_1) + R_{S,R}(x_1 + 2x_0, y_1). \tag{3}$$

The first two terms are on-axis autocorrelation terms, the correlation of reference and target signals with themselves; and the third and fourth terms are the correlations of the reference with the target.

Following the theoretical development for kth law nonlinearities put forth by Javidi[6] we find the output of the nonlinear system is made up of harmonics with the first harmonic having the correct phase information and highest intensity. The general equation of the output of the nonlinear system in the first harmonic is[6]

$$g_{1k}(U) = \frac{2\,\Gamma(k+1)\,\lfloor R(\alpha,\beta)\,S(\alpha,\beta)\rfloor^{k}}{\Gamma\!\left(1-\frac{1-k}{2}\right)\Gamma\!\left(1+\frac{1+k}{2}\right)}\;\cos\!\left[2x_0\,\alpha + \phi_S(\alpha,\beta) - \phi_R(\alpha,\beta)\right] \tag{4}$$

Assuming the objects were identical and using the hardclip nonlinearity (k = 0), this equation simplifies to

$$g_{10}(U) = \frac{4}{\pi}\cos(2x_0\,\alpha). \tag{5}$$

The Fourier transform of Eq. (5) results in the corresponding correlation term, which is an impulse function with amplitude $2/\pi$ located at $\pm\,2x_f$. Eq. (5) is similar to the light leaving the filter of a frequency plane correlator using an inverse filter.[6]

3. SYSTEM DESCRIPTION

The experimental correlator used for this study is a single SLM system shown in Figure 1. The SLM used is the Semetex magneto-optic spatial light modulator (MOSLM^{TM}) 128 x 128 pixel electrically addressed device. The input polarizer of the MOSLM was removed since the 10 mW He-Ne source was polarized 500:1. The MOSLM analyzer was replaced with a custom mount containing a polarizing beamsplitting cube in an effort to increase the device contrast ratio. The measured contrast ratio in the zeroth order varied from 7:1 to 70:1 over the active area of the device. The contrast ratio was more uniform with the first polarizer in place but did not increase beyond 70:1 and no significant improvement in correlation was observed. The MOSLM was placed behind the 40 cm Fourier transform lens to provide a variable scale factor similar to the front end of our compact correlator design.[10] The variable scale allows us to center and size the Fourier transform/correlation plane on the camera so the dc point of the first replicated Fourier transform order, due to the pixelated SLM, is just outside the field of view.[11] Under these conditions we knew the transform and correlation plane limits were the center 256 x 256 pixels of the 512 x 512 frame.

Previous analysis for the BJTC showed a high greylevel (beyond 8-bits) detector would be needed to adequately sample the low intensity Fourier components.[13] The argument was that the dc component in the Fourier plane is so large that the 256 greylevels in an 8-bit camera with linear response would be taken up in this peak, effectively making important higher frequency components zero, resulting in no correlation. Our computer simulations verify 256

---

[13] Javidi, B., Ruiz, J., and Ruiz, C. Effects of Fourier plane quantization on the performance of the binary nonlinear joint transform correlators, submitted to *Appl. Opt.*

greylevels are not sufficient to effect a correlation. These simulations were performed using a standard 2-D FFT algorithm and taking account to map the results to 256 levels as one would find in an experimental system.

We propose using a dc block to eliminate this high greylevel requirement problem. Our computer simulations and experimental results show the dc block allows the sensing of the higher Fourier components and good correlations are produced. The dc block was fashioned by exposing a holographic plate to a converging laser beam, developing, and placing it in the center of the Fourier plane. A 10 cm focal length lens is used as a 3:1 imaging relay to the Sony XC-37 CCD camera. This magnification is important for maintaining Nyquist sampling. The JPS consists of fringes which must be adequately sampled to produce results in the correlation step and whose period can be approximated using standard Bragg angle calculations. There must be at least one pixel per fringe sampling to correctly capture the JPS. The fringe period changes with object separation and must be magnified properly for all conditions to produce correlations. Our pixel to fringe sampling ratio varied from 4 to 11 depending on separation.

4. EXPERIMENTAL METHOD AND RESULTS

The binarized reference and target objects are placed on the MOSLM, the JPS is captured on the CCD camera and sent to a Zenith 248 AT computer. The center 256 x 256 pixels are extracted from this 512 x 512 frame and every other row and column is removed leaving a 128 x 128 array containing the JPS. As previously mentioned, the method of centering the JPS easily defined the correct area for extraction. Since we are oversampling the JPS from 4 to 11 times, removing the rows and columns to create the smaller array has no effect on the JPS data. The JPS is binarized around the global mean or median to determine which method performs best. The binarized signal is sent to the MOSLM and the correlation observed.

We placed neutral density filters ranging in value from 1 to 1.2 in front of the camera to capture the JPS, resulting in an equivalent laser power of 1 mW. Correlations performed using the global mean thresholding always yielded higher correlation peak intensity, higher peak-to-secondary (peak to next highest peak, typically greater than 7:1), and higher signal-to-noise ratio (SNR) than the global median binarization. We have no conclusions at this time why the mean performs best. The statistical conditions for the classic definition of SNR are not appropriate for real sensor imagery since it generally does not contain Gaussian, zero mean additive noise. We use a metric that accounts for this difference and is given by[14]

[14] Fielding, K., and Horner, J.L. (1989) Clutter effects of optical correlators, *Proceedings of the SPIE*, vol. 1151.

$$SNR = \frac{(C_0 - \bar{c})}{\sigma_{noise}}$$ (6)

where C_0 is the correlation peak intensity $\bar{c}$ and σ_{noise} are the average and standard deviation, respectively, of the data over the entire correlation plane excluding the peak itself. This is similar to that proposed by Dickey and Romero[15] and Kumar et al.[16] Using this metric, the SNR was greater than 60 for autocorrelations. The SNR falls off as the targets change in scale, in-plane rotation, and out-of-plane rotation as expected. If we subtract the average value from the correlation plane array, it is simple to show from Eq. (6) that

$$SNR = \frac{C_0'}{N_{rms}}$$ (7)

where C_0' and N_{rms} are now measured in the new zero mean correlation plane. This can easily be accomplished by capacitively coupling the photodetector used to read out the correlation plane data.

The objects used to study changes in separation, scale, in-plane rotation, and out-of-plane rotation are shown in Figure 2a. These models of an armored personnel carrier (APC) and tank were mounted on a rotation stage where accurate images of changes in rotations and scales were framegrabbed and stored in the computer. Constant lighting conditions were maintained to eliminate any errors in capturing and binarizing the data during collection. The objects in the final binarized imagery had values of 255 in a 0 background. We previously tried to use a commercial computer program to rotate and scale computer images, however, this technique produced poor correlation results. We attribute this to the distortion of the objects by the interpolation algorithm where many pixels that were part of the target would be turned off and others that were not part of the target would be turned on.

Figure 2b shows the binarized tanks placed together on the MOSLM generating the JPS seen in Figure 2c. The JPS binarized around the mean is shown in Figure 2d with the corresponding correlation shown in Figure 2e. The correlation in Figure 2e depicts the excellent measured peak-to-secondary of 10:1 and SNR of 67.

[15] Dickey, F.M., and Romero, L.A. (1989) Dual optimality of phase-only filter, *Opt. Lett.*, **14**:4.

[16] Kumar, B.V.K. V., Shi, W., and Hendrix C. Phase-only filters with maximally sharp correlation peaks, *Opt. Lett.*, under review Jan. 1990.
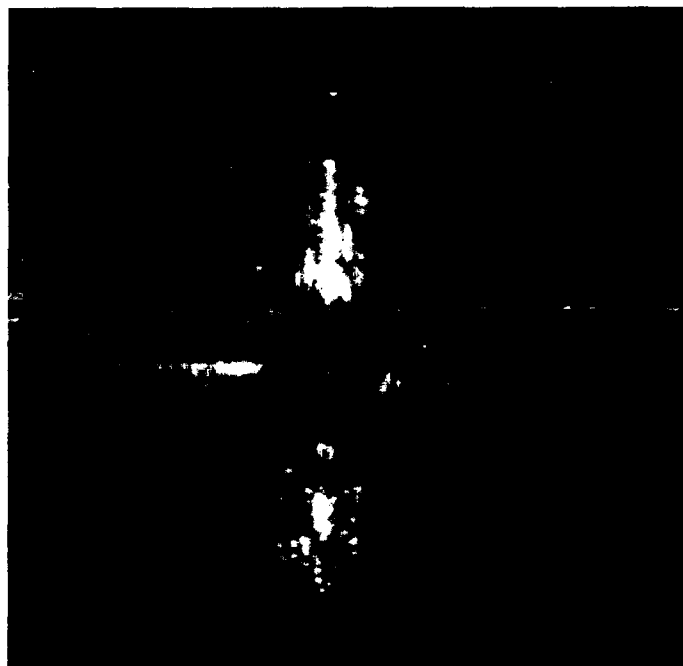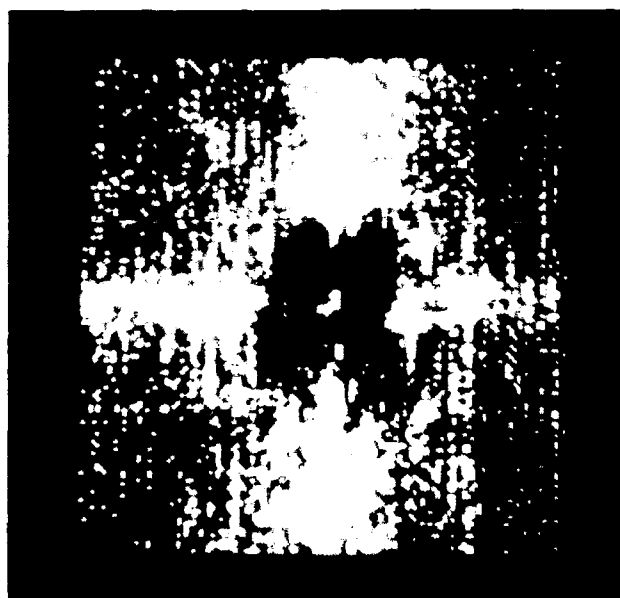
2 (a)

2(b)

Figure 2. (a) APC and Tank Model, (b) Binarized Tank, (c) JPS,
(d) Mean Binarized JPS, (e) Tank-Tank Correlations with DC Block
in Place.

8

2 (c)

2 (d)

2 (e)

4.1　Image Separation

Eq. (5) shows that the correlation peaks for objects separated by x_0 are located at $2x_0$. The peaks are twice as far from the SLM centerline as the objects themselves. When the objects are located half the distance from the centerline to the edge of the SLM, the corresponding correlations will be at the edge of the correlation plane. Any further separation puts the zeroth order correlation peaks into the first order correlation plane and vice versa. This is one disadvantage of using a pixelated device. Not only is the space bandwidth product limited by halving the device for target and reference; the space on each half is limited by the ultimate location of correlation peaks. The effect on the correlation peak intensity of object separation from the centerline is shown in Figure 3.
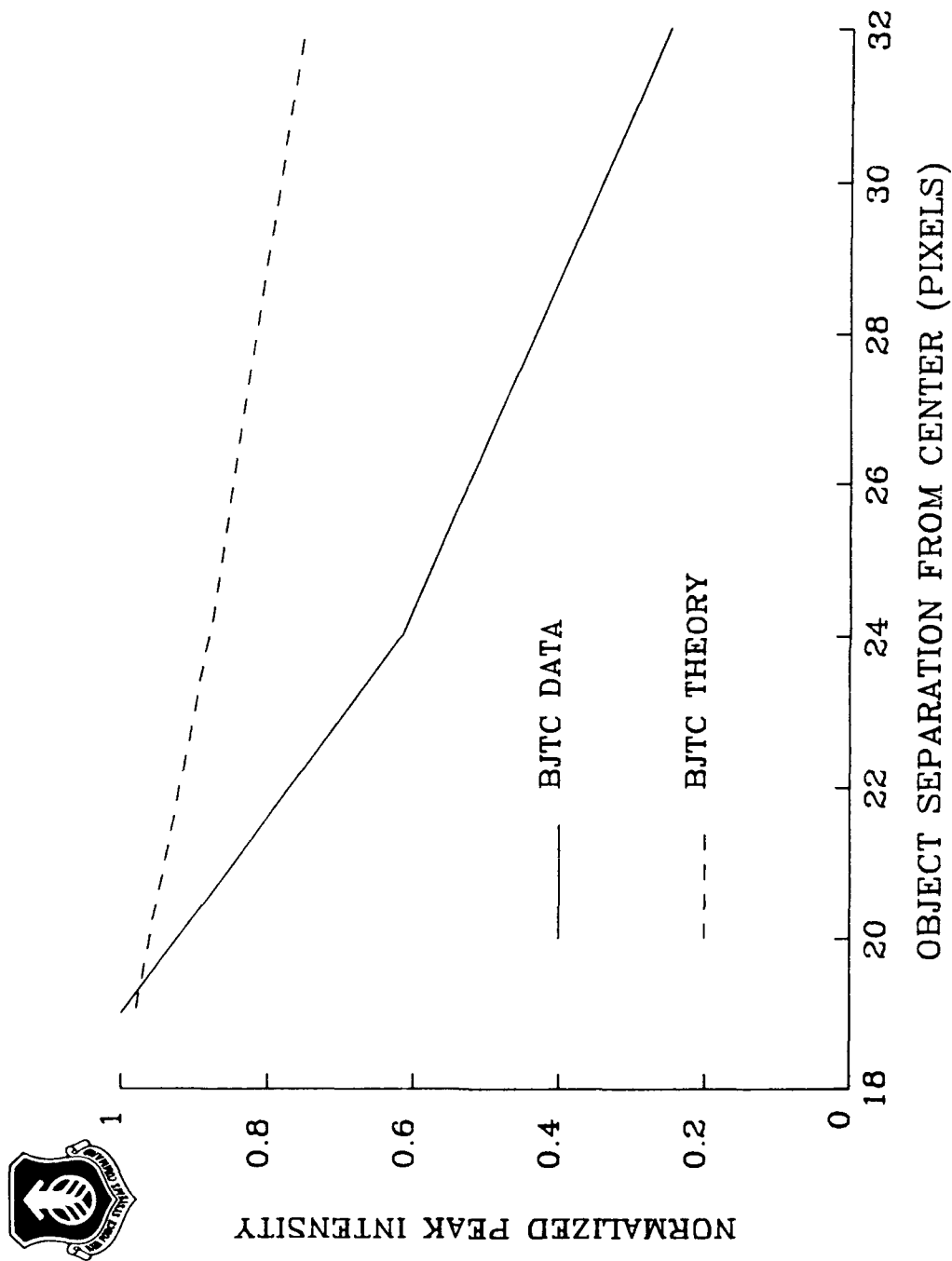
Figure 3. Normalized Peak Intensity vs Object Separation.

11

4.2 Image Distortion

The effects of in-plane rotation, out-of-plane rotation, and scale changes on the BJTC are shown in Figures 4a, 4b, and 4c. The experimental data is contrasted with computer simulations of the BJTC and a frequency plane correlator with the classical matched filter (CMF) using the same imagery.

These results show that the BJTC is much more sensitive than the CMF. In fact, the BJTC is more sensitive than the POF and BPOF whose graphs we have omitted for clarity.[17] The data verifies that the BJTC performs as an inverse filter which is the filter most sensitive to input distortions.[6]
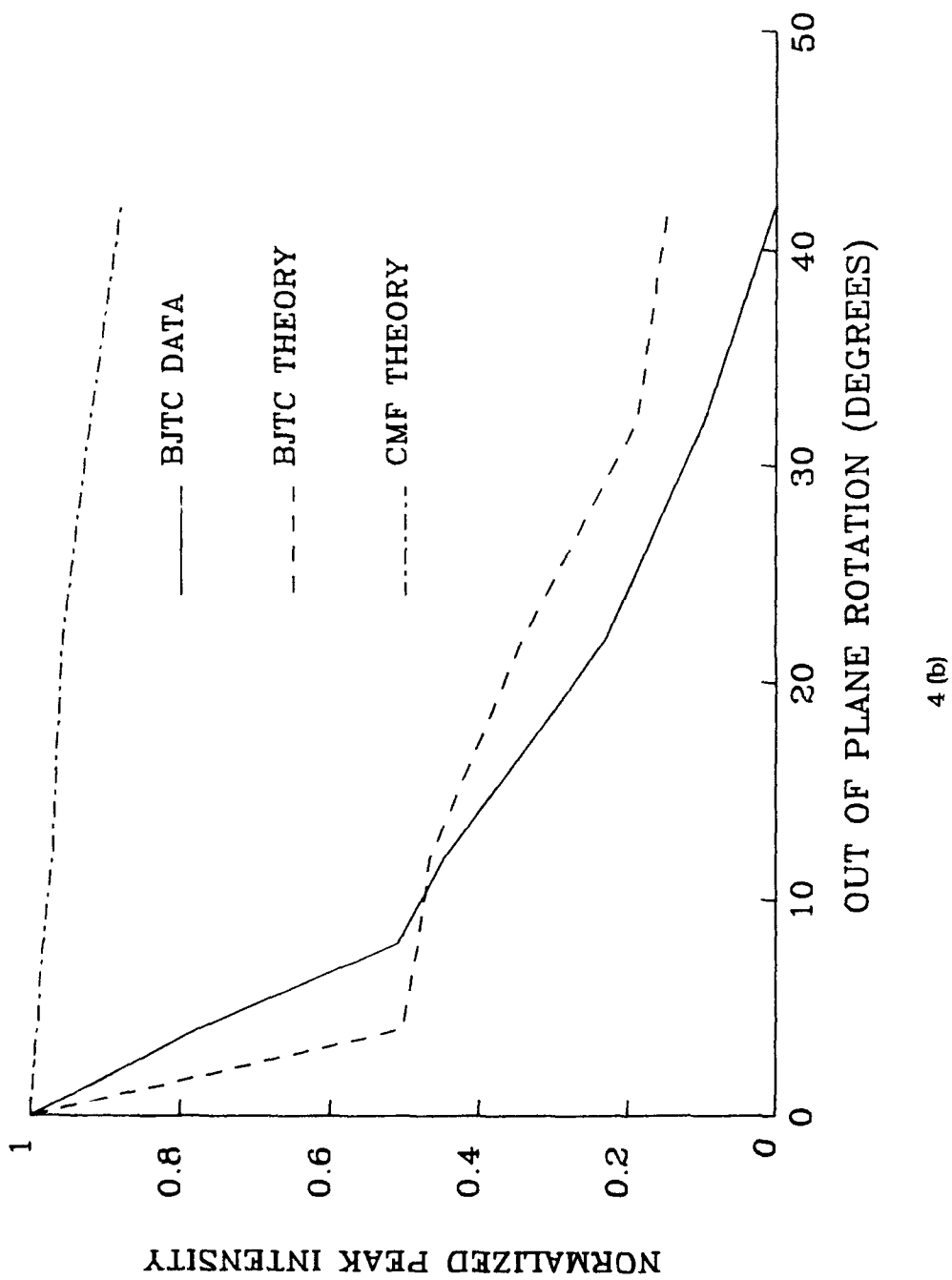
The above results pertain for autocorrelations. BJTC performance with objects that are not identical (cross-correlations) is examined next. Figure 5a shows the binarized APC and tank that are written to the MOSLM. The cross-correlation of these objects showing no distinct peak is seen in Figure 5b. The objects were chosen because they are similar and therefore show the superior discrimination ability of this system.
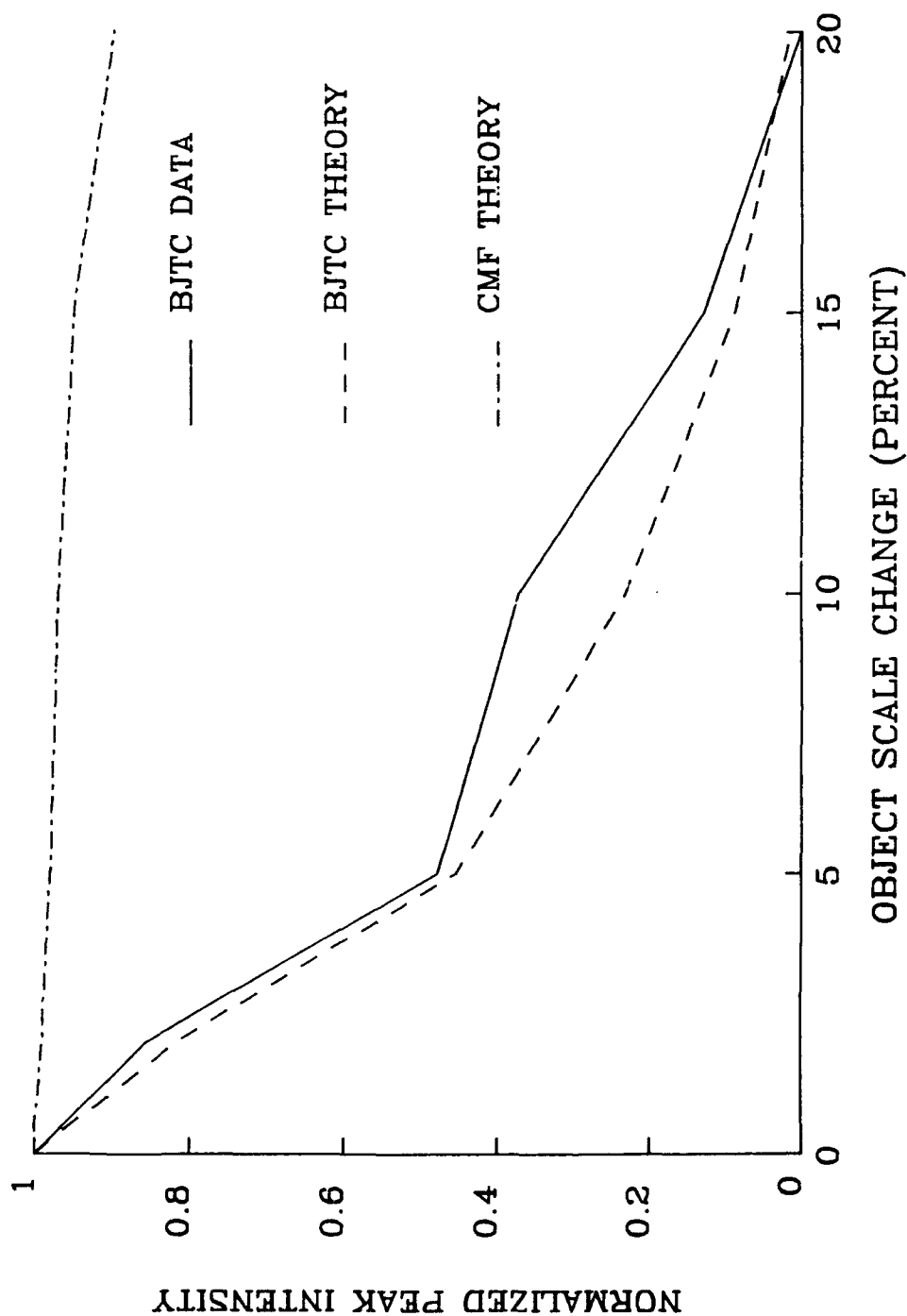
[17] Gianino, P. and Horner, J.L. (1984) Additional properties of the phase-only correlation filter. *Opt. Eng.*, **23**:695.
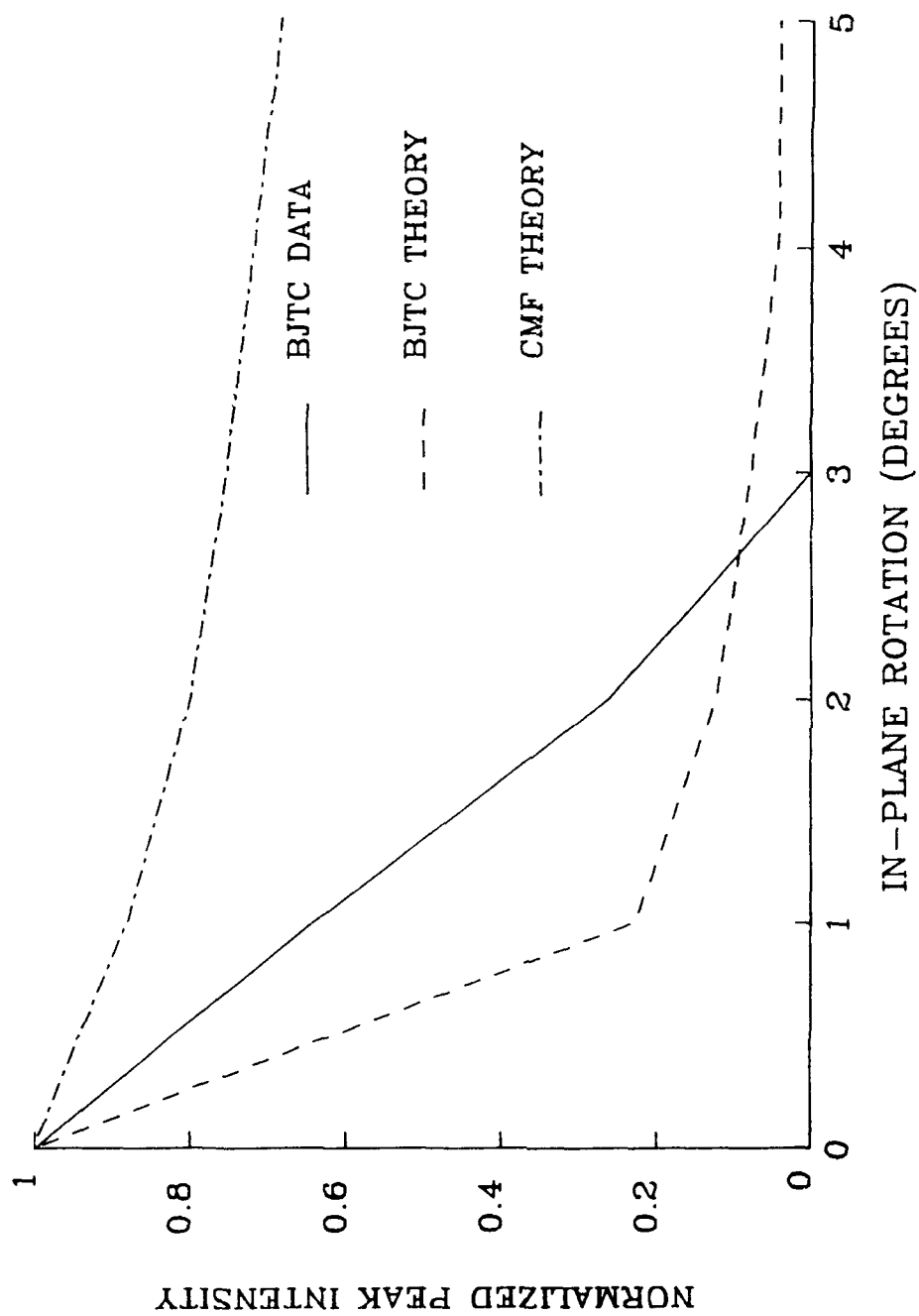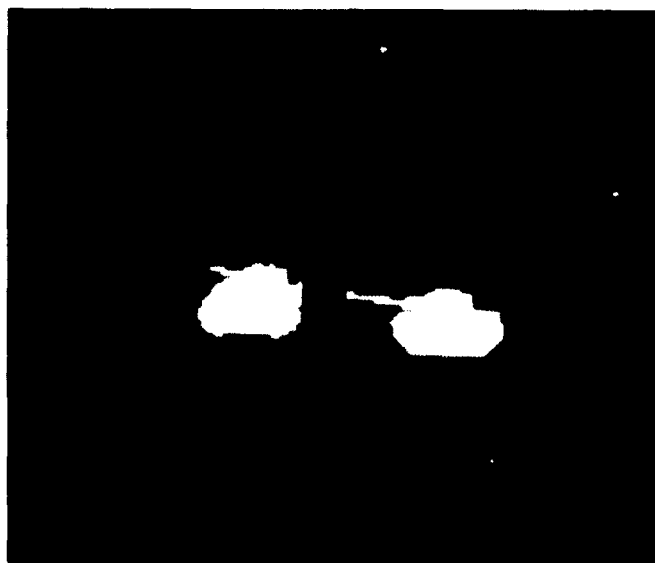
Figure 4. Normalized Peak Intensity vs (a) In-Plane Rotation. (b) Out-of-Plane Rotation, and (c) Scale.

OUT OF PLANE ROTATION (DEGREES)

4 (b)

NORMALIZED PEAK INTENSITY

BJTC DATA
BJTC THEORY
CMF THEORY

4 (c)

OBJECT SCALE CHANGE (PERCENT)

NORMALIZED PEAK INTENSITY

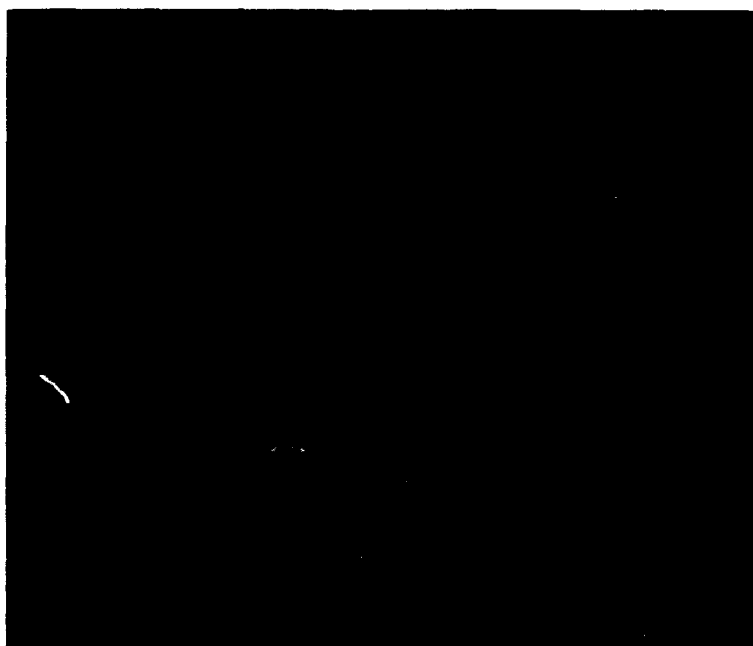BJTC DATA

BJTC THEORY

CMF THEORY

15

5 (a)

5 (b)

Figure 5. (a) Binarized APC and Tank Input, (b) Cross-Correlation.

16

4.3 Multiple Targets

Next we examine the BJTC performance using scenes containing multiple targets.[18] Figure 6a shows the input scene containing the tank (reference) and target tank and APC. Figure 6b is the corresponding correlation plane showing the good correlation of the tank and tank. Figure 6c is the input scene with one reference tank and three identical target tanks displaced on a diagonal. Note the similar diagonal structure in the correlation plane shown in Figure 6d. The correlations around the dc block are from target-target cross-correlations while those to the right and left are the correlation of the reference with each target. As seen in Figure 6d, we do not observe any of the false alarms predicted by the complicated JPS signal generated with the multiple objects.[19]

[18] Javidi, B., and Odeh, S. (1988) Multiple object identification by bipolar joint transform correlation, *Opt. Eng.*, **27**:295.

[19] Yu, F.T.S., Cheng, F., Nagata, T., and Gregory, D.A. (1989) Effects of fringe binarization of multiobject joint transform correlation, *Appl. Opt.*, **28**:2988.
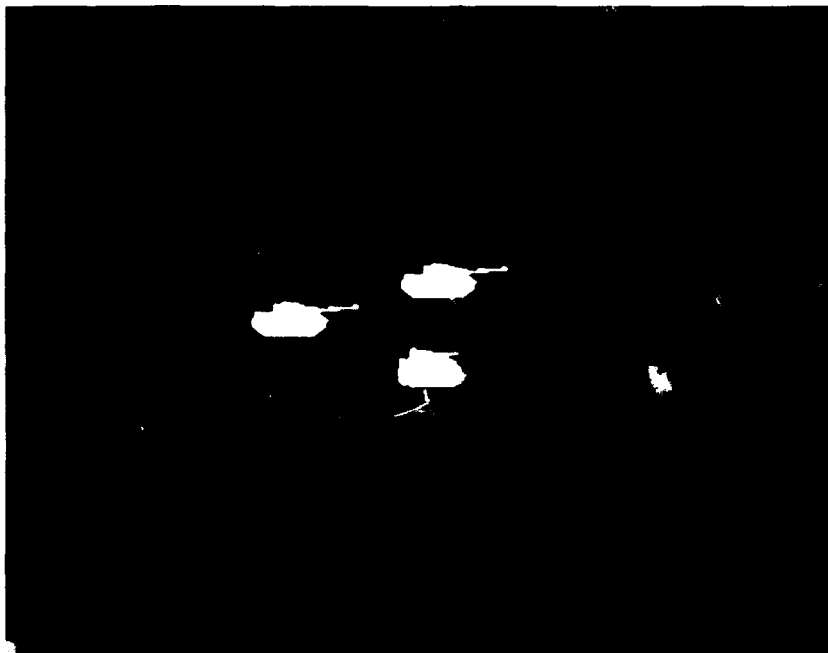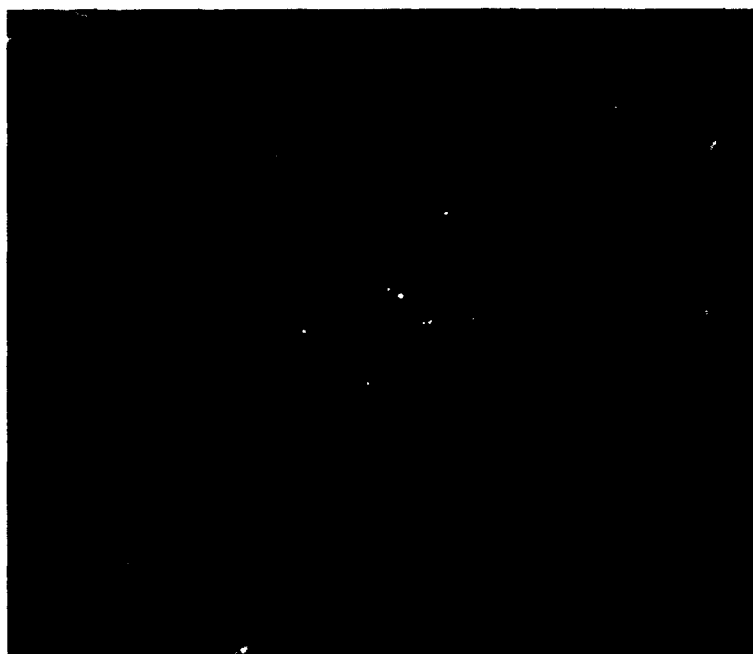
6 (a)

6 (b)

Figure 6. Multiple Target Experiments: (a) Tank Reference vs Tank and APC Targets, (b) Correlation Plane, (c) Tank Reference vs Three Identical Tank Targets, (d) Correlation Plane Showing Distinct Peaks for Each Target. The peaks near the dc block are target-target correlations.

18

6 (c)

4.4　Clutter Effects

The most complex and challenging task for any image identification system is to identify objects that are embedded in their natural or camoflaged surroundings. We will briefly describe the results of initial experimentation with cluttered imagery.

The cluttered input image shown in Figure 7a has a mean of 108 (on a scale of 0 to 255) and the imbedded object (tank) mean is 63. The tank is segmented out of the scene and used as the reference. A 55 x 64 pixel version of the entire scene is used as the target image. The reference and target were both binarized around the same threshold level varying from 45 to 100. Figures 7b, 7c, and 7d show the MOSLM inputs for threshold levels of 45, 75, and 85 respectively. Figures 8a and 8b show the correlations using JPS mean binarization for the input threshold levels of 45 and 85. Thresholding the inputs around 85 was the highest value that yielded correlations. This is approximately equal to the mean of the reference and target means. Figure 9 shows the effect on peak intensity as the input threshold level changes from 45 to 100.

In an operational system, the reference and target object illuminance will generally be different, presenting some complications which are not addressed here　Gregory et al analyzed and experimentally verified the existence of this problem.[20] We are working on a new input thresholding technique that will result in correlations as long as the mean of the target and background are not identical and we will deal with this effect in an upcoming publication.

[20]　Gregory, D.A., Loudin, J.A., and Yu, F.T.S. (1989) Illumination dependence of the joint transform correlation, Appl. Opt., **28**:3288.
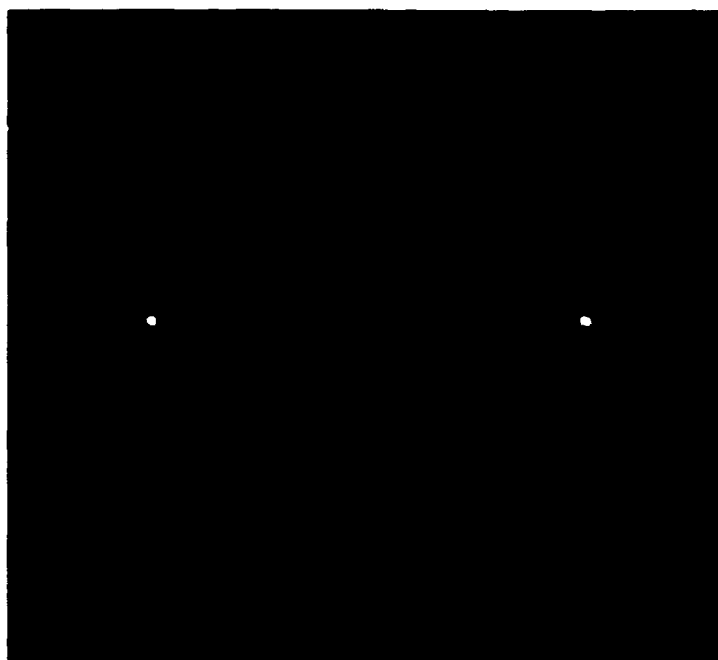
7 (a)

7 (b)

Figure 7. Clutter Experiments: (a) Clutter Scene; Reference and
Target Scene Thresholded and Binarized Around, (b) 45, (c) 75, and
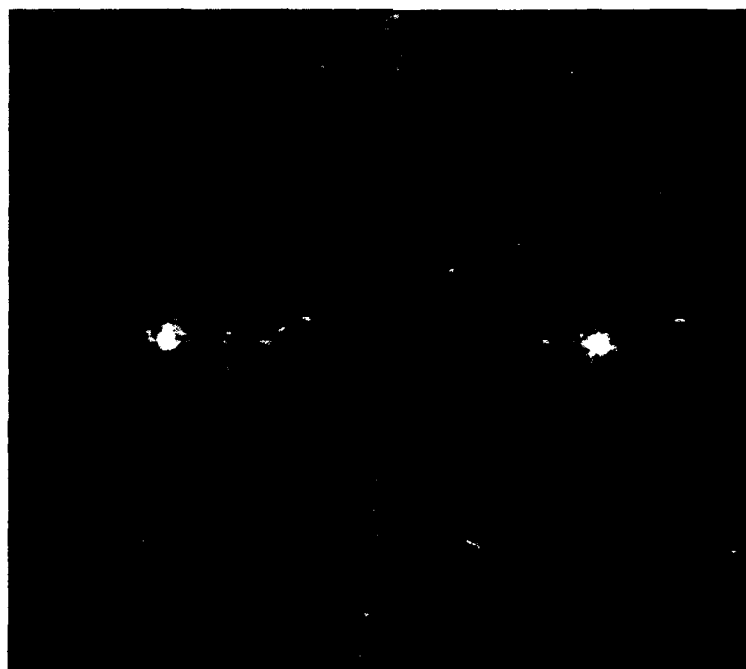(d) 85.

7 (c)

7 (d)

8 (a)

8 (b)

Figure 8. Clutter Correlation Results for Threshold Levels of (a) 45, and (b) 85.
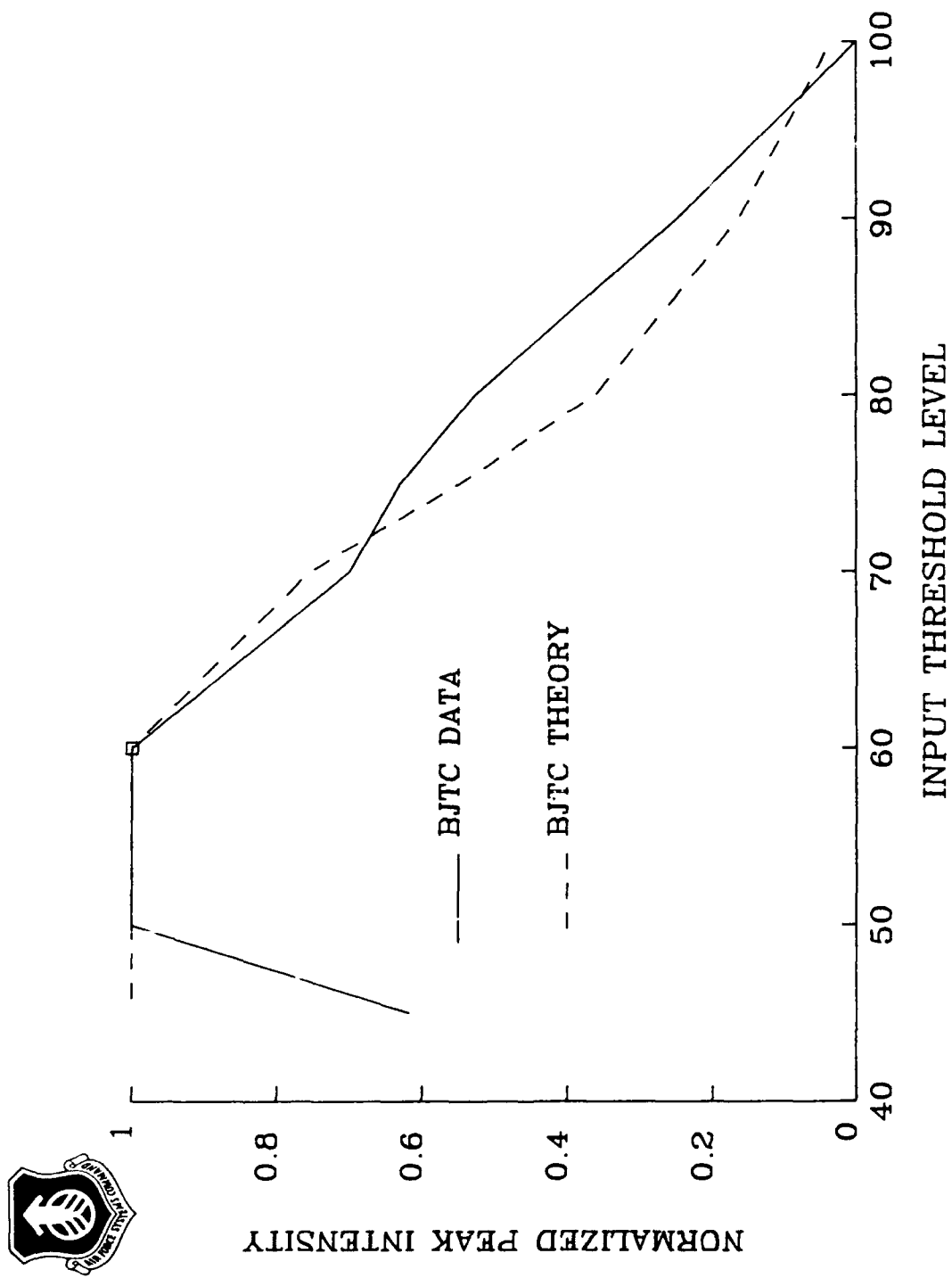
Figure 9. Normalized Peak Intensity vs Input Threshold Level.

5. CONCLUSIONS

The synthesis of several previous ideas has led to the system described here, a 1 focal length binary joint transform correlator using a dc block. The BJTC produces correlations with high peak-to-secondary and good signal-to-noise ratios. We have verified through experimentation that this system behaves as an inverse filter. The BJTC is much more sensitive than the CMF, POF, and BPOF to changes in separation, scale, in-plane rotation, and out-of-plane rotation. JPS binarization around the mean proves most effective.

The use of a dc block ensures the accurate capturing of the JPS for binarization with a standard 8-bit detector. We also found that this system does work without the dc block with the corresponding correlation peak intensity dropping 40-50 percent. Apparently, the large intensity values of the dc saturate but do not bloom onto the surrounding camera pixels, allowing the adequate capturing of the higher Fourier components, thereby producing reasonable correlations. The BJTC shows a good ability to identify multiple targets and targets in background clutter. More investigation is needed in this area.

References

1. Weaver, C.S., and Goodman, J.W. (1966) A technique for optically convolving two functions, *Appl. Opt.*, **5**:1248.

2. Florence, J. (1989) Joint-transform correlator systems using deformable-mirror spatial light modulators, *Opt. Lett.*, **14**:341.

3. Hudson, T. and Gregory, D. (1990) Joint transform correlation using an optically addressed ferro electric liquid crystal spatial light modulator, *Appl. Opt.*, **29**:1064.

4. Yu, F.T.S., Jutamulia, S., Lin, T.W., and Gregory, D.A. (1984) Adaptive real-time pattern recognition using a liquid crystal TV based joint transform correlator, *Appl. Opt.*, **26**:1370.

5. Javidi, B., and Kuo, C. (1988) Joint transform image correlation using a binary spatial light modulator at the Fourier plane, *Appl. Opt.*, **27**:663.

6. Javidi, B. (1989) Nonlinear joint power spectrum based optical correlation, *Appl. Opt.*, **28**:2358.

7. Javidi, B., and Horner, J.L. (1989) Multifunction nonlinear signal processor: deconvolution and correlation, *Opt. Eng.*, **28**:837.

8. Javidi, B., and Horner, J.L. (1989) Single spatial light modulator joint transform correlator, *Appl. Opt.*, **28**:1027.

9. Javidi, B., Gregory, D.A., and Horner, J.L. (1989) Single spatial light medulator joint transform correlator architectures, *Appl. Opt.*, **28**:411.

10. Makekau, C., and Horner, J.L. (1990) 2-f optical correlator, *Appl. Opt.*, **29**.

11. Goodman, J.W. (1968) *Introduction to Fourier Optics*, McGraw-Hill, San Francisco.

12. Vander Lugt, A. (1966) Practical considerations for the use of spatial carrier-frequency filter, *Appl. Opt.*, **5**:1760.

13. Javidi, B., Ruiz, J., and Ruiz, C. Effects of Fourier plane quantization on the performance of the binary nonlinear joint transform correlators, submitted to *Appl. Opt.*

14. Fielding, K., and Horner, J.L. (1989) Clutter effects of optical correlators, *Proceedings of the SPIE*, vol. 1151.

15. Dickey, F.M., and Romero, L.A. (1989) Dual optimality of phase-only filter, *Opt. Lett.*, 14:4.

16. Kumar, B.V.K. V., Shi, W., and Hendrix C. Phase-only filters with maximally sharp correlation peaks, *Opt. Lett.*, under review Jan. 1990.

17. Gianino, P. and Horner, J.L. (1984) Additional properties of the phase-only correlation filter, *Opt. Eng.*, 23:695.

18. Javidi, B., and Odeh, S. (1988) Multiple object identification by bipolar joint transform correlation, *Opt. Eng.*, 27:295.

19. Yu, F.T.S., Cheng, F., Nagata, T., and Gregory, D.A. (1989) Effects of fringe binarization of multiobject joint transform correlation, *Appl. Opt.*, 28:2988.

20. Gregory, D.A., Loudin, J.A., and Yu, F.T.S. (1989) Illumination dependence of the joint transform correlation, *Appl. Opt.*, 28:3288.

MISSION
of
Rome Air Development Center

RADC plans and executes research, development, test and selected acquisition programs in support of Command, Control, Communications and Intelligence (C³I) activities. Technical and engineering support within areas of competence is provided to ESD Program Offices (POs) and other ESD elements to perform effective acquisition of C³I systems. The areas of technical competence include communications, command and control, battle management, information processing, surveillance sensors, intelligence data collection and handling, solid state sciences, electromagnetics, and propagation, and electronic, maintainability, and compatibility.